

An adaptive subset simulation algorithm for system reliability analysis with discontinuous limit states

Jianpeng Chan, Iason Papaioannou, Daniel Straub

Engineering Risk Analysis Group, Technische Universität München, Arcisstr. 21, 80290 München, Germany

Abstract

Many system reliability problems involve performance functions with a discontinuous distribution. Such situations occur in both connectivity- and flow-based network reliability problems, due to binary or multi-state random variables entering the definition of the system performance or due to the discontinuous nature of the system model. When solving this kind of problems, the standard subset simulation algorithm with fixed intermediate conditional probability and fixed number of samples per level can lead to substantial errors, since the discontinuity of the output can result in an ambiguous definition of the sought percentile of the samples and, hence, of the intermediate domains. In this paper, we propose an adaptive subset simulation algorithm to determine the reliability of systems whose performance function is a discontinuous random variable. The proposed algorithm chooses the number of samples and the intermediate conditional probabilities adaptively. We discuss two MCMC algorithms for generation of the samples in the intermediate domains, the adaptive conditional sampling method and a novel independent Metropolis-Hastings algorithm that efficiently samples in discrete input spaces. The accuracy and efficiency of the proposed algorithm are demonstrated by a set of numerical examples.

Keywords: Subset simulation, System reliability analysis, Limit state function with discontinuous distribution, Conditional sampling, independent Metropolis-Hastings

1. Introduction

Infrastructure networks, such as power grids and water supply systems, deliver essential services to society. Failures of such networks can have severe consequences. Quantification of the probability of survival or, conversely, the probability of failure of such systems is essential in understanding and managing their reliability; this is the main purpose of network system reliability assessment.

For reliability analysis purposes, the performance of the system can be assessed by the limit state function (LSF), also known as performance function or structure function, $g(\mathbf{X})$. \mathbf{X} is an n -dimensional vector of random variables with joint cumulative distribution function (CDF) $F_{\mathbf{X}}$ and represents the uncertainty in the model input. By convention, failure of the system occurs for all system states \mathbf{x} for which $g(\mathbf{x}) \leq 0$. The probability of failure of the system is defined as

$$p_f \triangleq \mathbb{P}(g(\mathbf{X}) \leq 0) = \int_{g(\mathbf{x}) \leq 0} dF_{\mathbf{X}}(\mathbf{x}) \quad (1)$$

The vector of basic random variables \mathbf{X} entering the definition of the LSF of network systems usually contains discrete random variables, which results in a LSF with discontinuous distribution. This is due to the fact that the performance of the network is often calculated through a function of a large number of binary or multi-state components. Moreover, real-world infrastructure networks are often designed to be highly reliable. This leads to high-dimensional reliability assessment problems with small failure probabilities [1].

Network performance is often measured through connectivity or 'travel time' (or flow) [2]. In connectivity-based problems, one evaluates the probability that a given set of nodes are connected, given that each component of the network fails with some probability. Typically, both the system performance and the component state are modeled as binary random variables. In this context, $g(\mathbf{X})$ is known as the structure function [3]. **A set of sampling-based methods have been proposed for such kind of problems (e.g., [4, 5, 6, 7, 8, 9, 10, 11]), and a comparative study can be found in [12, 13].**

In this paper, we focus on flow-based problems where the system performance and/or the component are typically modeled as multi-state or continuous random variables instead of binary ones, and, hence, most of the sampling techniques tailored for connectivity-based problems cannot be implemented

35 directly. One of the major concerns in this area is the maximum flow that a
 36 stochastic network can deliver, i.e., the probability that the maximum flow
 37 from one or more source nodes to one or more terminal nodes is less than a
 38 predefined demand level. **A number of sampling based methods have been**
 39 **proposed for this type of problems [14, 15, 16, 17, 18, 19, 20, 21, 22].** How-
 40 ever, all these methods assume that the edge capacities are independent and
 41 discrete random variables, which is often unrealistic. [1] employs the stan-
 42 dard subset simulation (SuS) algorithm [23] to efficiently solve maximum-flow
 43 reliability problems, where both the edge capacity and the network perfor-
 44 mance are modeled as continuous random variables. [24] use the standard
 45 SuS algorithm in reliability analysis of gas pipelines. However, as discussed
 46 in this paper, the adaptive approach of the standard SuS for determining the
 47 intermediate levels is not suitable for LSFs with discontinuous distribution,
 48 which is the case for most network reliability problems. As an example, Fig.
 49 1 shows the CDF of the LSF of the IEEE39 bus benchmark system (described
 in Section 5.4). The CDF is discontinuous with 'jumps'. To overcome this

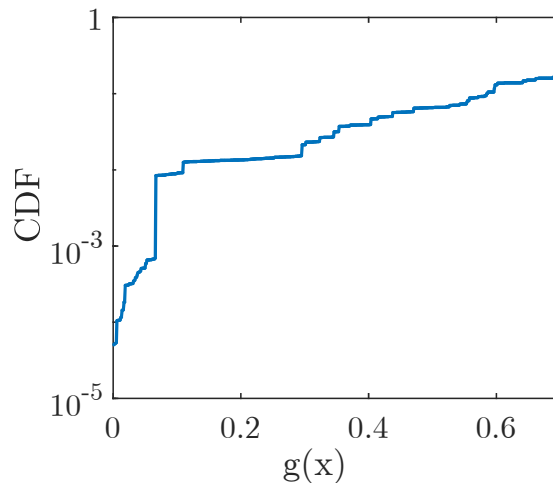


Figure 1: CDF of the LSF of the IEEE39 bus benchmark system of Section 5.4

50
 51 limitation, one may construct a problem equivalent to the original one but
 52 with LSFs with continuous distribution, and then use SuS to solve this equiv-
 53 alent problem. This approach has been explored by Ching and Hsu [2] for
 54 connectivity-based problems, where a virtual random walk model is solved
 55 to get a continuous proxy of the original binary connectivity. Typically, such
 56 transformations need to be derived for the problem at hand.

57 The generalized splitting method [25] has also been employed to solve both
 58 connectivity- [10] and flow-based problems [26] in combination with tailored
 59 and efficient Gibbs samplers. It should be stressed that the determination of
 60 the intermediate levels in the generalized splitting method is through a pilot
 61 run of the adaptive multilevel splitting algorithm [25, 10, 27], which is essen-
 62 tially the standard SuS algorithm. Therefore, transformation of discontinu-
 63 ously distributed LSF to continuous one is also needed for these approaches.
 64 The basic idea of SuS is to express the probability of failure as a product of
 65 larger conditional probabilities of a set of intermediate nested events. Two
 66 ingredients of the SuS algorithm are essential for obtaining an accurate and
 67 efficient estimator. The first is the efficient simulation of conditional samples,
 68 which is achieved through Markov Chain Monte Carlo (MCMC) methods
 69 [23, 28]. The second is the proper choice of the intermediate events. Simi-
 70 larly to the cross entropy method [29, 30], the intermediate failure events in
 71 SuS are chosen adaptively, so that the estimates of the conditional probabili-
 72 ties equal a predefined value p_0 . This is achieved through generating a fixed
 73 number of samples in each conditional level, sorting the samples according
 74 to their LSF values and determining the p_0 -percentile of the samples, which
 75 is set as the threshold defining the next intermediate failure event. When
 76 solving network reliability problems, the discontinuous nature of the LSF can
 77 result in a large number of samples in a certain conditional level having the
 78 same LSF value. In such cases, the standard SuS method will result in an
 79 ambiguous definition of the intermediate domains. In extreme conditions,
 80 all samples generated in a certain level might have the same LSF value, in
 81 which case the sample process can get stuck and might not reach the failure
 82 domain.

83 To address this issue, we introduce a novel variant of SuS called *adaptive*
 84 *effort subset simulation* (aE-SuS) method. Our method chooses the number
 85 of samples per level and the respective conditional probability adaptively
 86 to ensure that an adequate number of samples fall in the subsequent inter-
 87 mediate domain. Compared with other non-sampling based methods (e.g.,
 88 [31, 32, 33, 34, 35]), the proposed method facilitates using advanced deter-
 89 ministic network analysis algorithms considering complex network dynamics
 90 like cascading failure. On the other hand, owing to its sampling nature, the
 91 aE-SuS algorithm may require a large number of simulations to achieve an ac-
 92 ceptable result. It should be stressed that the proposed aE-SuS algorithm is
 93 applicable for dependent input random variables and any MCMC algorithm
 94 that enables efficient sampling of the intermediate conditional distributions

95 can be combined with the proposed algorithm.
 96 The paper is organized as follows: Section 2 gives a brief introduction to the
 97 standard SuS. Section 3 discusses two MCMC algorithms in the context of
 98 network reliability assessment. Section 4 introduces the basic idea as well as
 99 the implementation details of the aE-SuS method. In Section 5, the perfor-
 100 mance of the proposed algorithm is illustrated by a set of numerical examples,
 101 a one-dimensional multi-state problem, a multidimensional flow-based prob-
 102 lem with combined continuous and binary capacities, a binomial experiment
 103 with small success probability, and a benchmark power transmission network
 104 system. The paper closes with the conclusions in Section 6.

105 2. Standard subset simulation

106 2.1. Brief introduction of subset simulation

107 The basic idea of SuS is to express the rare failure event $F = \{\mathbf{x} :$
 108 $g(\mathbf{x}) \leq 0\}$ as the intersection of a sequence of nested intermediate events
 109 $F_1 \supset F_2 \supset \dots \supset F_m$. Owing to the nestedness of the intermediate events,
 110 the failure event can be expressed as $F = \bigcap_{l=1}^m F_l$. The failure probability can
 111 then be decomposed as the following product of conditional probabilities:

$$\mathbb{P}(F) = \prod_{l=1}^m \mathbb{P}(F_l | F_{l-1}) \quad (2)$$

112 where F_0 is the certain event. Ideally, the intermediate events are selected
 113 such that each conditional probability is large, typically ≥ 0.1 . In this way,
 114 the original problem of estimating a small probability is transformed to a
 115 sequence of m intermediate problems of evaluating larger conditional proba-
 116 bilities.

117 The estimation of each conditional probability $\mathbb{P}(F_l | F_{l-1})$ requires sampling
 118 from the distribution of the random variables conditional on F_{l-1} , denoted as
 119 $Q(\cdot | F_{l-1})$, where $Q(\cdot | F_0)$ represents the initial input distribution and equals
 120 the generalized derivative of the input CDF $F_{\mathbf{X}}(\cdot)$. $Q(\cdot | F_0)$ can be sampled
 121 by standard Monte Carlo sampling, but the distributions $Q(\cdot | F_l), l > 0$, are
 122 only known point-wise up to a normalizing constant and, hence, cannot be
 123 sampled directly. Therefore MCMC sampling is employed. The sampling
 124 process in the l -th conditional sampling level is performed as follows: (1)
 125 Select the samples $\mathcal{P}^{(l-1)}$ from the $(l-1)$ -th level that fall in F_l as the seeds
 126 $\mathcal{S}^{(l)}$ ($\mathcal{P}^{(0)}$ is generated through Monte Carlo sampling). (2) From each seed,

127 start a Markov chain that has the target distribution $Q(\cdot|F_l)$ as the station-
 128 ary distribution, and record all the states as new samples $\mathcal{P}^{(l)}$. (3) Take
 129 the samples $\mathcal{P}^{(l)}$ located in F_{l+1} as new seeds $\mathcal{S}^{(l+1)}$ and estimate $\mathbb{P}(F_{l+1}|F_l)$
 130 as $\frac{|\mathcal{S}^{(l+1)}|}{|\mathcal{P}^{(l)}|}$ where $|\mathcal{S}^{(l+1)}|$ and $|\mathcal{P}^{(l)}|$ denote the number of seeds and samples,
 131 respectively. The above three steps are repeated successively until F is ap-
 132 proached. We note that the number of the samples per level $|\mathcal{P}^{(l)}|$ is usually
 133 fixed prior to the analysis.

134 Defining the intermediate events a priori is typically challenging. Hence, in
 135 standard SuS the intermediate failure events are chosen adaptively during
 136 the simulation such that each conditional probability equals a predefined
 137 constant p_0 . This standard SuS approach is also termed (fixed effort) adap-
 138 tive multilevel splitting [25]. In this variant, step (3) in the above sampling
 139 process is modified as follows: Order the samples $\mathcal{P}^{(l)}$ by their LSF val-
 140 ues. The first p_0 -percent of these sorted samples are then taken as seeds
 141 for the next sampling level and the LSF value of the p_0 -percentile b_{l+1} is
 142 used to define the boundary of the next intermediate domain, such that
 143 $F_{l+1} = \{\mathbf{x} : g(\mathbf{x}) \leq b_{l+1}\}$. The resulting SuS estimator of the probability of
 144 failure is given as:

$$\hat{p}_f = p_0^{m-1} \frac{N_f}{N} \quad (3)$$

145 where N and N_f represent the number of samples and failure samples at final
 146 level, respectively. The standard SuS algorithm is summarized in Algorithm
 147 1.

148 As previously mentioned, MCMC sampling is applied to generate samples
 149 from each conditional distribution $Q(\cdot|F_l)$. In SuS, the seeds $\mathcal{S}^{(l)}$ already
 150 follow approximately the target distribution [23], hence, a burn-in period is
 151 not considered in practice. Since the samples generated from the same seed
 152 are states of the same Markov chain, they will be dependent; their correla-
 153 tion depends on the autocorrelation function of the underlying Markov chain.
 154 The stronger the correlation between samples, the larger the variance of the
 155 estimates of the conditional probabilities. Additionally, samples that share
 156 the same history, namely, their Markov chains are branches with root at the
 157 same Monte Carlo sample, will be correlated, even when they are in different
 158 levels. Such correlation introduces a dependency of the conditional proba-
 159 bility estimators, which further increases the variance of the SuS estimator.
 160 Hence, the quality of the final probability estimate strongly depends on the
 161 particular choice and setting of the MCMC algorithm.

Algorithm 1: SuS algorithm

Input: $p_0 \in (0, 1)$, an integer N multiple of $\frac{1}{p_0}$

- 1 $l \leftarrow 0, b_l \leftarrow \inf$
- 2 **while** $b_l > 0$ **do**
- 3 **if** $l = 0$ **then**
- 4 Generate N samples $\{\mathbf{x}_k\}_{k=1}^N$ from the initial distribution
 $Q(\cdot|F_0)$
- 5 **else**
- 6 Generate N samples $\{\mathbf{x}_k\}_{k=1}^N$ from the target distribution
 $Q(\cdot|F_l)$ with an MCMC algorithm with seeds $\mathcal{S}^{(l)}$
- 7 Sort $\{\mathbf{x}_k\}_{k=1}^N$ by increasing order of their LSFs $g(\cdot)$, and denote
 the sorted samples as $\{\bar{\mathbf{x}}_k\}_{k=1}^N$
- 8 $b_{l+1} \leftarrow g(\bar{\mathbf{x}}_{p_0 \cdot N})$
- 9 **if** $b_{l+1} \leq 0$ **then**
- 10 $b_{l+1} \leftarrow 0$
- 11 $N_f = \sum_{k=1}^N \mathbb{I}\{g(\bar{\mathbf{x}}_k) \leq 0\}$
- 12 Take the $\mathcal{S}^{(l+1)} \triangleq \{\bar{\mathbf{x}}_k\}_{k=1}^{p_0 \cdot N}$ as the seeds for the next level
- 13 $l \leftarrow l + 1$
- 14 $\hat{p}_f \leftarrow p_0^{l-1} \frac{N_f}{N}$

Output: \hat{p}_f

163 *2.2. Accuracy of the Subset Simulation estimator*

164 The accuracy of the SuS estimator of the probability of failure \hat{p}_f can be
 165 assessed by the mean-square error, which is decomposed as:

$$\text{MSE}(\hat{p}_f) = (p_f - \mathbb{E}(\hat{p}_f))^2 + \text{Var}(\hat{p}_f) \quad (4)$$

166 The first term on the right-hand side of Eq.(4) represents the bias contribu-
 167 tion and the second term the variance of the SuS estimator.

168 Assume first that the intermediate events are defined before the simulation.
 169 In the Monte Carlo level ($l = 0$), samples $\mathcal{P}^{(0)}$ are generated from $Q(\cdot|F_0)$
 170 independently, and therefore the seeds $\mathcal{S}^{(1)}$ follow the distribution $Q(\cdot|F_1)$.
 171 This will lead to so-called perfect sampling when simulating the Markov
 172 chains in the next level. Since the chains have already reached the stationary
 173 state at the beginning, no burn-in time is needed, and all samples $\mathcal{P}^{(1)}$ will
 174 follow $Q(\cdot|F_1)$. In this way, samples $\mathcal{P}^{(l)}$ generated in any l -th conditional
 175 level will follow the target distribution $Q(\cdot|F_l)$ and the corresponding esti-
 176 mator of the conditional probability $\hat{p}(F_{l+1}|F_l)$ will be unbiased. Moreover,
 177 [25] proves that the resulting failure probability estimator \hat{p}_f is also unbiased
 178 if both intermediate events and length of the Markov chain are predefined,
 179 i.e., if they are independent of the simulation process.

180 Since the intermediate events are selected adaptively in SuS, samples $\mathcal{S}^{(l)}$
 181 will not completely follow the target distribution. As a result, both condi-
 182 tional probability estimator and failure probability estimator will be slightly
 183 biased. Nevertheless, compared to the variance of the estimator, the squared
 184 bias is one order of magnitude smaller [23] and, hence, its contribution to
 185 the mean-square error (MSE) of the estimator is negligible. In other words,
 186 the error of the SuS is mainly due to the variance of the failure probability
 187 estimator rather than the bias. The most common and reliable way to calcu-
 188 late the variance $\text{Var}(\hat{p}_f)$ is to run SuS several times and to use the sample
 189 variance as the unbiased estimation of the $\text{Var}(\hat{p}_f)$. One can also evaluate
 190 the variance approximately through a single run of the SuS. More details can
 191 be found in [23] and [28]. However, this approximate estimator is shown to
 192 underrepresent the true variance of \hat{p}_f , especially for small target p_f .

193 **3. Markov Chain Monte Carlo algorithm for network reliability**
 194 **assessment**

195 Most MCMC algorithms that are widely used in risk analysis can be
 196 regarded as variants of the Metropolis-Hastings (M-H) algorithm. These in-
 197 clude, for example, Gibbs sampling [10][26], conditional sampling [28] and
 198 Hamiltonian Monte Carlo [36]. To sample from the intermediate target dis-
 199 tribution $Q(\cdot|F_l)$ in SuS, M-H algorithm proceeds in the following two steps
 200 [28]:

- 201 1. Generate a candidate sample \mathbf{v} from the distribution $Q_p^{(l)}(\cdot|\mathbf{x}_k)$ which
- 202 is termed the proposal distribution.
- 203 2. Accept or reject \mathbf{v} .

$$204 \quad \mathbf{x}_{k+1} = \begin{cases} \mathbf{v}, & \text{with prob. } \alpha \\ \mathbf{x}_k, & \text{with prob. } 1 - \alpha \end{cases} \quad \text{where}$$

$$205 \quad \alpha = \mathbb{I}\{\mathbf{v} \in F_l\} \min \left\{ 1, \frac{Q(\mathbf{v}|F_0)Q_p^{(l)}(\mathbf{x}_k|\mathbf{v})}{Q(\mathbf{x}_k|F_0)Q_p^{(l)}(\mathbf{v}|\mathbf{x}_k)} \right\}$$

206 It can be shown that the M-H algorithm satisfies the detailed balance condi-
 207 tion independent of the choice of the proposal distribution. In this section, we
 208 first discuss the adaptive conditional sampling method of [28] in the context
 209 of network reliability assessment and then propose a more efficient yet less
 210 general independent M-H algorithm, which is applicable in problems with
 211 discrete input spaces.

212 *3.1. Adaptive conditional sampling in standard normal space*

213 *3.1.1. Implementation in standard normal space*

214 Let \mathbf{U} denote an n -dimensional random vector that has the indepen-
 215 dent standard normal distribution. The original random vector \mathbf{X} can be
 216 expressed in terms of the vector \mathbf{U} through an isoprobabilistic mapping
 217 $\mathbf{T} : \mathbb{R}^n \rightarrow \mathbb{R}^n$. One can define the reliability problem in the \mathbf{U} -space as
 218 follows:

$$p_f = \mathbb{P}(g(\mathbf{X}) \leq 0) = \mathbb{P}(G(\mathbf{U}) \leq 0) = \int_{G(\mathbf{u} \leq 0)} \varphi_n(\mathbf{u}) d\mathbf{u} \quad (5)$$

219 where $G(\mathbf{U}) = g(\mathbf{T}(\mathbf{U}))$ and $\varphi_n(\mathbf{u})$ is the n -dimensional independent stan-
 220 dard normal joint probability density function (PDF). The mapping $\mathbf{T}(\cdot)$

221 can be obtained by the Rosenblatt transformation, which is implemented as
 222 follows:

$$\begin{aligned}
 x_1 &= F_{X_1}^{-1}(\Phi(u_1)) \\
 x_2 &= F_{X_2}^{-1}(\Phi(u_2)|x_1) \\
 &\vdots \\
 x_n &= F_{X_n}^{-1}(\Phi(u_m)|x_1, \dots, x_{n-1})
 \end{aligned}
 \tag{6}$$

223 where Φ represents the CDF of standard normal distribution and $F_{X_d}(\cdot|x_1, \dots, x_{d-1})$
 224 denotes the conditional CDF of X_d given $X_1 = x_1, \dots, X_{d-1} = x_{d-1}$. If any
 225 subset of \mathbf{X} consists of discrete random variables, then it is possible that the
 226 functions $F_{X_d}(\cdot|x_1, \dots, x_{d-1})$ are not strictly invertible. Therefore, we use
 227 the following extended definition of the inverse of a CDF

$$F^{-1}(a) = \inf(x : F(x) \geq a) \tag{7}$$

228 We note that in such cases the Rosenblatt transformation is not one-to-one
 229 and hence, the inverse mapping from \mathbf{X} to \mathbf{U} is not uniquely defined.

230 3.1.2. Adaptive conditional sampling algorithm

231 Having defined the transformation from the original \mathbf{X} -space to the \mathbf{U} -
 232 space, SuS can be used to solve the reliability problem in the transformed
 233 space. At the l -th level of SuS, MCMC sampling is applied to sample from
 234 the conditional standard normal density $p_U(\cdot|F_l)$. Sampling according to
 235 this density can be performed by application of the aCS algorithm. Before
 236 describing the aCS algorithm, we first discuss its non-adaptive variant, the
 237 standard conditional sampling (CS) algorithm. The transition from the cur-
 238 rent state \mathbf{u}_k to a new state \mathbf{u}_{k+1} using CS is as follows: First, a candidate
 239 \mathbf{v} is generated. The CS sampler imposes that the candidate and the current
 240 state are jointly Gaussian with standard normal marginal distribution $\varphi_n(\cdot)$
 241 and predefined symmetric cross-correlation matrix, \mathbf{R} . One then samples \mathbf{v}
 242 from the joint Gaussian distribution conditional on the current state, i.e.,
 243 from $\mathcal{N}(\mathbf{v}; \mathbf{R}\mathbf{u}_k, \mathbf{I} - \mathbf{R}\mathbf{R}^T)$, where \mathbf{I} is the identity matrix. The candidate is
 244 accepted if it is located in the intermediate failure domain F_l , in which case
 245 it is set as the new state \mathbf{u}_{k+1} . Otherwise, \mathbf{u}_k is taken as the new state. CS
 246 can be summarized as follows:

- 247 1. Generate candidate sample \mathbf{v} from the normal distribution $\mathcal{N}(\mathbf{v}; \mathbf{R}\mathbf{u}_k, \mathbf{I} -$
 248 $\mathbf{R}\mathbf{R}^T)$.

249 2. Accept or reject \mathbf{v} .

$$250 \quad \mathbf{u}_{k+1} = \begin{cases} \mathbf{v}, & \mathbf{v} \in F_l \\ \mathbf{u}_k, & \mathbf{v} \notin F_l \end{cases}$$

251 It can be proven that the above transition satisfies the detailed balance con-
252 dition with respect to the target distribution $p_{\mathbf{U}}(\cdot|F_l)$, hence, $p_{\mathbf{U}}(\cdot|F_l)$ is the
253 stationary distribution of the generated Markov chain [28, 37]. In fact, CS
254 can be regarded as the M-H sampler with proposal distribution taken as
255 $\mathcal{N}(\mathbf{v}; \mathbf{R}\mathbf{u}_k, \mathbf{I} - \mathbf{R}\mathbf{R}^T)$ [28]. We further note that the CS sampler will never
256 generate repeated candidates, which results in an acceptance probability that
257 is independent of the dimension of the vector \mathbf{U} . Hence, it is suitable for
258 application to high-dimensional problems.

259 The performance of the CS sampler depends on the choice of the matrix \mathbf{R}
260 or, equivalently, the covariance matrix of the proposal distribution \mathcal{N} . Usua-
261 lly, \mathbf{R} is chosen as a diagonal matrix with d -th diagonal term equal to ρ_d ,
262 which implies a component-wise sampling scheme, i.e., the d -th component
263 of candidate, v_d , is sampled from $\mathcal{N}(v_d; \rho_d u_{k,d}, 1 - \rho_d^2)$. Large values of ρ_d
264 lead to strong correlation between current and next state, but small values
265 also lead to increased correlation due to the high rejection rate in the second
266 step of CS. The correlation of the generated Markov chains can be con-
267 trolled by choosing ρ_d or, equivalently, the standard deviation $\sigma_d = \sqrt{1 - \rho_d^2}$
268 adaptively, employing intermediate results from the simulation. In adaptive
269 MCMC algorithms, the chain correlation is usually controlled by matching
270 a near-optimal acceptance probability of the chain [38]. The aCS algorithm
271 [28] adapts the sampling parameters by running batches of N_a chains start-
272 ing from randomly selected seeds. After running each batch, the acceptance
273 probability is estimated and the sampling parameters are adapted to match
274 a pre-defined acceptance probability α^* . The aCS algorithm for generating
275 N samples according to $p_{\mathbf{U}}(\cdot|F_l)$ starting from seeds $\mathcal{S}^{(l)}$ is given in Appendix
276 A.

277 3.2. Independent Metropolis-Hastings algorithm

278 In network reliability assessment, the probability content at the inter-
279 mediate domains in SuS typically centers at multiple discrete system states
280 (modes) and, hence, the intermediate target distribution is multimodal. To
281 efficiently sample from such distribution, we propose a novel independent M-
282 H algorithm. The algorithm is applicable when all input random variables
283 are discrete and exploits the information of the discarded samples in previous

284 sampling levels to form a proper proposal distribution in the M-H algorithm
 285 that is independent of the current state of the chain. Specifically, let \mathcal{X}_l rep-
 286 resent the set of samples discarded at level l , in other words, the generated
 287 samples at level l that are not in the $(l + 1)$ -th intermediate domain. The
 288 proposal distribution $Q_p^{(l)}(\mathbf{x})$ of the M-H algorithm at level l is then defined
 289 as the original input distribution $Q(\mathbf{x}|F_0)$ excluding the states visited by the
 290 previously discarded samples. That is,

$$Q_p^{(l)}(\mathbf{x}) \propto Q(\mathbf{x}|F_0) \mathbb{I}\{\mathbf{x} \notin \cup_{i=0, \dots, l-1} \mathcal{X}_i\} \quad (8)$$

291 Since all samples in $\cup_{i=0, \dots, l-1} \mathcal{X}_i$ are located outside the intermediate domain
 292 F_l , F_l is included in the support of the proposal distribution, $\Omega_p^{(l)} = \mathbf{x} \notin$
 $\cup_{i=0, \dots, l-1} \mathcal{X}_i$. This is illustrated in Fig. 2. Moreover, the proposal distribution

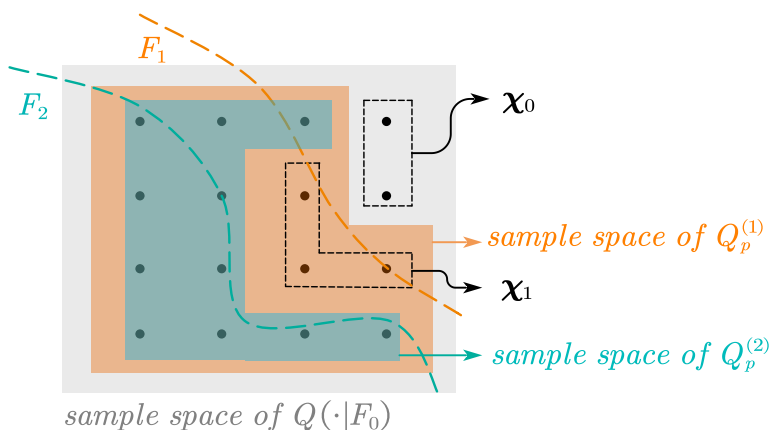


Figure 2: Schematic diagram of proposal distributions. (The black dots represent the basic random events, and the dotted curve indicates the intermediate failure domain)

293
 294 has exactly the same shape as the intermediate target distribution in F_l as
 295 they are both proportional to the input distribution $Q(\mathbf{x}|F_0)$. The acceptance
 296 rate α of the candidate generated by this proposal is given as

$$\alpha = \mathbb{I}\{\mathbf{x} \in F_l\} \min \left\{ 1, \frac{Q(\mathbf{x}|F_0)Q(\mathbf{x}_k|F_0)}{Q(\mathbf{x}_k|F_0)Q(\mathbf{x}|F_0)} \right\} = \mathbb{I}\{\mathbf{x} \in F_l\} \quad (9)$$

297 Note that both the generation and the acceptance of the candidate are inde-
 298 pendent of the current state. In the literature, M-H samplers whose proposal
 299 distribution is independent of the current state are termed independent M-H
 300 samplers. We note that the samples generated by this algorithm are not

301 independent, since we get a repeated sample when rejecting the candidate.
 302 This is the main difference between the independent M-H algorithm and
 303 rejection sampling with envelope $\frac{1}{\mathbb{E}[\alpha]}Q_p^{(l)}(\mathbf{x})$, which generates independent
 304 samples [39]. In the latter, one gets a new sample only when the candidate
 305 is accepted and, hence, the computational cost of rejection sampling is much
 306 higher than the independent M-H algorithm especially as the mean accep-
 307 tance rate $\mathbb{E}[\alpha]$ is small. The average acceptance probability, $\mathbb{E}[\alpha]$, can be
 308 calculated through dividing $\mathbb{P}(\mathbf{X} \in F_l)$ by $\mathbb{P}(\mathbf{X} \notin \cup_{i=0,\dots,l-1}\mathcal{X}_i)$, i.e.,

$$\mathbb{E}_{Q_p^{(l)}}[\alpha] = \frac{\mathbb{P}(\mathbf{X} \in F_l)}{\mathbb{P}(\mathbf{X} \notin \cup_{i=0,\dots,l-1}\mathcal{X}_i)} \quad (10)$$

309 The magnitude of $\mathbb{E}[\alpha]$ tends to decrease as the intermediate level goes higher.
 310 Additionally, the sample size at each level, the dimension of the problem and
 311 the input distribution will also influence the mean acceptance rate $\mathbb{E}[\alpha]$. The
 312 influence is investigated in detail through a binomial experiment in Section
 313 5.

314 The implementation of the above independent M-H algorithm is relatively
 315 simple and can be performed in the following two steps:

- 316 1. Generate candidate sample \mathbf{v} from the proposal distribution $Q_p^{(l)}(\mathbf{x})$.
- 317 2. Accept or reject \mathbf{v} .

$$318 \quad \mathbf{x}_{k+1} = \begin{cases} \mathbf{v}, \mathbf{v} \in F_l \\ \mathbf{x}_k, \mathbf{v} \notin F_l \end{cases}$$

319 To sample from the proposal distribution, $Q_p^{(l)}(\mathbf{x})$, one can sample directly
 320 from the input distribution and keep those samples that differ from the pre-
 321 vious discarded samples. However such process can be quite inefficient when
 322 the proposal distribution is far from the input distribution, for instance, at
 323 deep intermediate levels. Such issue can be circumvented by applying the
 324 bound-based sampling algorithm [12], given that the input random variables
 325 are multivariate categorical distributed. Details on this algorithm can be
 326 found in Appendix B.

327 4. Adaptive effort subset simulation method

328 In each conditional level l of the SuS method with fixed number of samples
 329 per level and adaptive estimation of the intermediate events, the p_0 -percentile
 330 of the LSF values of the samples $\mathcal{P}^{(l)}$, b_{l+1} , is used to define the boundary

331 of the intermediate domain. This adaptive approach works well when only
 332 a few samples are located on the boundary $g(\mathbf{x}) = b_{l+1}$, i.e., a few samples
 333 have the same LSF value as the p_0 -percentile. However, it can happen that
 334 many samples fall on this boundary, particularly in the following cases:

- 335 (1) \mathbf{X} includes discrete random variables.
- 336 (2) The LSF is defined such that the probability measure of the set $\{\mathbf{x} :$
 337 $g(\mathbf{x}) = b_{l+1}\}$ is strictly greater than zero.
- 338 (3) The parameters of the MCMC algorithm are inappropriately set, re-
 339 sulting in the candidates being rejected successively many times.

340 While case (3) can be avoided by an appropriate implementation of the
 341 MCMC algorithm, cases (1) and (2) are common in the context of network
 342 reliability assessment. This will result in an ambiguous definition of the in-
 343 termediate domain F_{l+1} and can lead to an inaccurate estimate of the failure
 344 probability. In extreme situations, all samples generated in a certain level
 345 will have the same LSF value and the adaptive sampling process can get
 346 stuck and never reach the failure domain.

347 In this section, we modify the standard SuS algorithm to circumvent this
 348 problem. The resulting algorithm modifies the adaptive selection of the in-
 349 termediate domains and adapts the number of samples per level (sampling
 350 effort) throughout the simulation. We term the proposed approach aE-SuS.
 351 As will be made clear, these modifications enable application of the method to
 352 general network reliability problems. The proposed algorithm is introduced
 353 in the following and summarized in Algorithm 2.

354 4.1. Intermediate domains

355 In order to provide a clear (unambiguous) definition of the intermediate
 356 domains, one can apply the following adaptive approach. At each conditional
 357 level, generate a set of samples $\mathcal{P}^{(l)}$ and define a temporary event F_{temp} as
 358 $\{\mathbf{x} : g(\mathbf{x}) \leq b_{l+1}\}$ where b_{l+1} is the p_0 -percentile of the LSF values of $\mathcal{P}^{(l)}$.
 359 If $F_{temp} = F_l$, define the next intermediate event F_{l+1} as $\{\mathbf{x} : g(\mathbf{x}) < b_{l+1}\}$,
 360 otherwise set $F_{l+1} = F_{temp}$. This approach guarantees that $F_{l+1} \subsetneq F_l$, which
 361 avoids a degeneracy of the sampling process.

362 Because of the discrete nature of $g(\mathbf{x})$, it might be difficult to check whether
 363 $F_{temp} = F_l$ or not when $F_l = \{\mathbf{x} : g(\mathbf{x}) < b_l\}$. Therefore, we check if
 364 $b_{l+1} = \max\{g(\mathbf{x}) : \mathbf{x} \in \mathcal{P}^{(l)}\}$ instead. The latter condition checks whether
 365 the p_0 percentile of the LSF values equals the maximum LSF value of the
 366 samples $\mathcal{P}^{(l)}$, and is a necessary (but not sufficient) condition of $F_{temp} = F_l$.

367 Note that $F_{l+1} \subsetneq F_l$ still remains true after this modification, since $F_l/$
368 $F_{l+1} \neq \emptyset$ and contains at least the samples taking the maximum LSF value
369 in $\mathcal{P}^{(l)}$. The above adaptive approach for choosing the intermediate domains
370 is described in lines 11-20 of Algorithm 2.

371 4.2. Sampling at the intermediate levels

372 The approach for selecting the intermediate domains, introduced in Sec-
373 tion 3.1, could potentially lead to a very small number of failure samples
374 per level, which reduces the accuracy of the estimates of the intermediate
375 conditional probabilities. We hence need to adapt the number of samples
376 per level to ensure that these estimates remain accurate. We first calculate
377 the number of samples that fall into the domain F_{l+1} (the number of seeds
378 N_s). If this number is smaller than a predefined constant C , we increase
379 the current sampling effort N_c and append $\mathcal{P}^{(l)}$ with N new samples. De-
380 note the extended sample set as $\mathcal{P}_{\text{ext}}^{(l)}$. The new samples should also follow
381 the target distribution $Q(\cdot|F_l)$, and hence approximately $\mathbb{P}(F_{l+1}|F_l)$ of these
382 samples should be located in F_{l+1} . Therefore, one needs to further generate
383 $N = N_c \cdot \frac{C - N_s}{N_s}$ samples to get approximately C seeds, which is shown in line
384 22 of Algorithm 2. Note that $N > 0$ always holds. In the algorithm, the con-
385 stant C is taken as a predefined proportion $tol \in (0, 1)$ of $p_0 \cdot N_0$, the product
386 of initial conditional probability and the initial sample size. Larger tol will
387 lead to more accurate but less efficient result. We have found $tol \in (0.5, 0.8)$
388 to be a good choice for the investigated cases.

389 In practice, the above appending process may need to be iterated several
390 times to achieve at least C seeds. For a fixed F_{l+1} , with every iteration and
391 increasing number of samples, the number of the seeds will keep increasing
392 until the desired threshold C is achieved. By doing this, even in the extreme
393 case where all the samples in $\mathcal{P}^{(l)}$ have the same LSF value, the sampling
394 process will keep moving forward towards the failure domain and will no
395 longer get stuck in this level as in the standard SuS algorithm.

396 To append new samples which follow the target distribution $Q(\cdot|F_l)$, we pro-
397 pose to extend the Markov chains generated in the initial intermediate sam-
398 pling step ($iter = 0$, in Algorithm 2). This is illustrated in Fig. 3. As shown
399 in the figure, for each seed in $\mathcal{S}^{(l)}$, a Markov chain is constructed in the 0th
400 iteration. The last sample (tail) of this chain is then taken as the seed for the
401 chain in the next iteration. The transition distribution of the chain remains
402 unchanged. The above process may be iterated several times and is described
403 as Algorithm 3. For iteration $it = 0, \dots$, the input of Algorithm 3 consists

404 of 4 values: the number of samples to append N , the number of Markov
405 chains $N_{ch} = |\mathcal{S}^{(l)}|$, the transition distribution of each chain $\{\Gamma_i\}_{i=1}^{N_{ch}}$, which
406 is determined by the target distribution $Q(\cdot|F_l)$ and the employed MCMC
407 algorithm, and the seed for each chain $\{\mathbf{e}_i^{(it)}\}_{i=1}^{N_{ch}}$, which is taken as $\mathcal{S}^{(l)}$ when
408 $it = 0$ and otherwise as the tail of the Markov chains from the previous iter-
409 ation $\{\mathbf{t}_i^{(it-1)}\}_{i=1}^{N_{ch}}$. The output of the algorithm is N new generated samples
410 $\mathcal{P}_{\text{new}}^{(l)}$ and the tail (last sample) of each chain $\{\mathbf{t}_i^{(it)}\}_{i=1}^{N_{ch}}$.

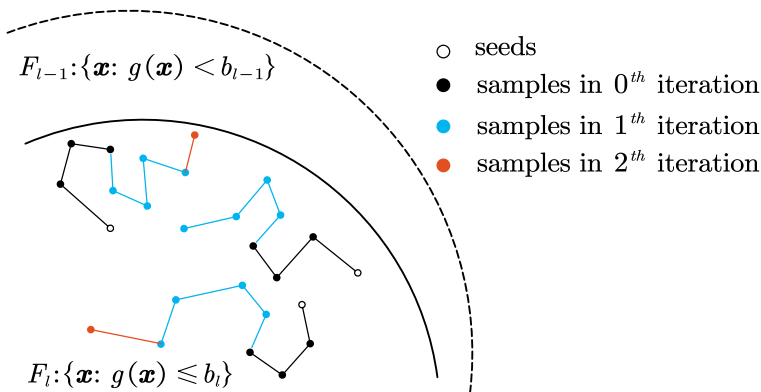


Figure 3: Schematic diagram of the appending method.

411

412 5. Examples

413 5.1. Multistate random variable

414 Consider a discrete random variable X with 7 states $\{x_1, \dots, x_7\}$. We
415 consider two cases. In case 1, the CDF of X , $F_X(\cdot)$, is set such that $\frac{F_X(x_{i+1})}{F_X(x_i)} \leq$
416 10, while in case 2, there is a big 'jump' between the third and the fourth
417 state, i.e., $\frac{F_X(x_4)}{F_X(x_3)} \approx 599$. The CDF of X for the two considered cases is given
418 in Table 1 and is illustrated in Fig 4. The LSF is defined as $g(X) = X + 5$
419 such that the failure probability $\mathbb{P}(X \leq -5)$ equals 10^{-5} for both cases.

420 We implement SuS and the proposed aE-SuS respectively in standard normal
421 space to evaluate the failure probability and compare them with crude MCS.
422 The MCMC algorithm is aCS. For SuS, the sampling effort is fixed to 1,000,
423 and the conditional probability is 0.1. For aE-SuS, the parameters are set to
424 be $tol = 0.5$, $N_0 = 1,000$, $p_0 = 0.1$. Each method is run 1,000 times to get the
425 relative bias, coefficient of variation and average computational cost of the

Algorithm 2: Adaptive effort subset simulation algorithm

Input: $tol \in (0, 1)$, $p_0 \in (0, 1)$, an integer N_0 multiple of $1/p_0$
 1 $l \leftarrow 0, b_l \leftarrow \inf, N \leftarrow N_0, \mathcal{P}^{(l)} \leftarrow \emptyset$
 2 **while** $b_l > 0$ **do**
 3 $iter \leftarrow 0, N_s \leftarrow 0$
 4 **while** $N_s < tol \cdot N_0 \cdot p_0$ **do**
 5 **if** $l = 0$ **then**
 6 Generate N samples $\{\mathbf{x}_k\}_{k=1}^N$ from the initial distribution
 $Q(\cdot|F_0)$ and add them to $\mathcal{P}^{(l)}$
 7 **else**
 8 Generate N samples $\{\mathbf{x}_k\}_{k=1}^N$ from the target distribution
 $Q(\cdot|F_l)$ with appending algorithm and add them to $\mathcal{P}^{(l)}$
 9 $N_c \leftarrow |\mathcal{P}^{(l)}|$ // total sample size
 10 Sort the elements of $\mathcal{P}^{(l)}$ by increasing order of their LSF
 values $g(\mathbf{x})$, and denote the sorted samples as $\{\bar{\mathbf{x}}_k\}_{k=1}^{N_c}$
 11 **if** $iter = 0$ **then**
 12 $b_{l+1} \leftarrow g(\bar{\mathbf{x}}_{p_0 \cdot N_0})$
 13 **if** $b_{l+1} \leq 0$ **then**
 14 $b_{l+1} \leftarrow 0$
 15 $N_s \leftarrow \sum_{k=1}^{N_c} \mathbb{I}\{g(\bar{\mathbf{x}}_k) \leq b_{l+1}\}, F_{l+1} \triangleq \{\mathbf{x} : g(\mathbf{x}) \leq b_{l+1}\}$
 16 Break
 17 **else if** $b_{l+1} < g(\bar{\mathbf{x}}_{N_c})$ **then**
 18 $N_s \leftarrow \sum_{k=1}^{N_c} \mathbb{I}\{g(\bar{\mathbf{x}}_k) \leq b_{l+1}\}, F_{l+1} \triangleq \{\mathbf{x} : g(\mathbf{x}) \leq b_{l+1}\}$
 19 Break
 20 $N_s \leftarrow \sum_{k=1}^{N_c} \mathbb{I}\{g(\bar{\mathbf{x}}_k) < b_{l+1}\}, F_{l+1} \triangleq \{\mathbf{x} : g(\mathbf{x}) < b_{l+1}\}$
 21 **if** $N_s < tol \cdot N_0 \cdot p_0$ **then**
 22 $N \leftarrow \lceil N_c \cdot \frac{tol \cdot N_0 \cdot p_0}{\max(1, N_s)} \rceil - N_c \geq 1$
 23 $iter \leftarrow iter + 1$
 24 Take the $\mathcal{S}^{(l+1)} \triangleq \{\bar{\mathbf{x}}_k\}_{k=1}^{N_s}$ as the seeds for the next level
 25 $N \leftarrow N_0 - N_s, \mathcal{P}^{(l+1)} \leftarrow \mathcal{S}^{(l+1)}, l \leftarrow l + 1$
 26 $\hat{p}(F_l|F_{l-1}) \leftarrow \frac{N_s}{N_c}$
 27 $\hat{p}(F) \leftarrow \prod_{j=1}^l \hat{p}(F_j|F_{j-1})$
Output: $\hat{p}(F)$

Algorithm 3: Appending algorithm

Input: $N, N_{ch}, \{\Gamma_i\}_{i=1}^{N_{ch}}, \{\mathbf{e}_i^{(it)}\}_{i=1}^{N_{ch}}$
 1 Randomly choose $\text{mod}(N, N_{ch})$ elements from the set $\{1, 2, \dots, N_{ch}\}$, say χ
 2 $\mathcal{P}_{\text{new}}^{(l)} \leftarrow \emptyset$
 3 **for** $i = 1, \dots, N_{ch}$ **do**
 4 **if** $i \in \chi$ **then**
 5 $j \leftarrow \lfloor \frac{N}{N_{ch}} \rfloor + 1$
 6 **else**
 7 $j \leftarrow \lfloor \frac{N}{N_{ch}} \rfloor$
 8 $\mathbf{x}_0 \leftarrow \mathbf{e}_i^{(it)}$
 9 **for** $k = 1, \dots, j$ **do**
 10 Sample \mathbf{x}_k from transition density $\Gamma_i(\cdot | \mathbf{x}_{k-1})$
 11 Add \mathbf{x}_k to $\mathcal{P}_{\text{new}}^{(l)}$
 12 $\mathbf{t}_i^{(it)} \leftarrow \mathbf{x}_j$
Output: $\mathcal{P}_{\text{new}}^{(l)}, \{\mathbf{t}_i^{(it)}\}_{i=1}^{N_{ch}}$

426 failure probability estimator. The results for case 1 and case 2 are shown in
 427 Tables 2 and 3 respectively. In both cases, aE-SuS shows good accuracy, a
 428 negligible bias and a much smaller coefficient of variation than crude MCS.
 429 We note that the coefficient of variation of crude MCS is given for the same
 430 computational effort as the proposed aE-SuS method. In contrast, SuS gives
 431 a strongly biased estimate of the failure probability with high coefficient of
 432 variation in the first case and falls into a dead loop in the second case.

Table 1: CDF of X for Example 5.1.

State	-6	-4	-3	-2	-1	0	1
CDF(case1)	1e-5	1e-4	1e-3	1e-2	1e-1	5e-1	1
CDF(case2)	1e-5	3e-5	5e-5	3e-2	1e-1	5e-1	1

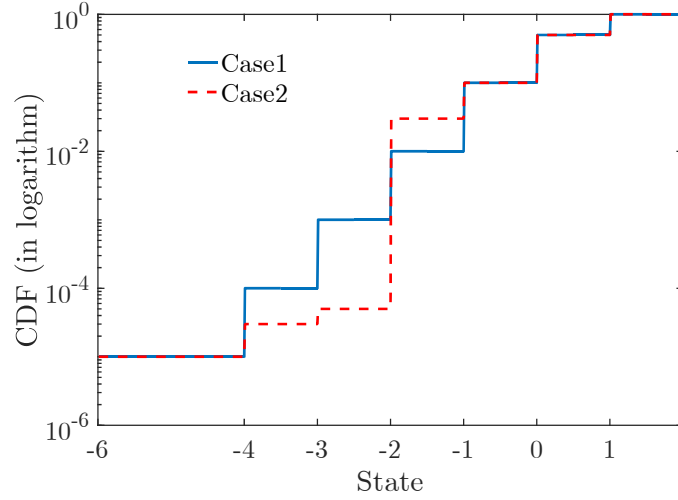


Figure 4: CDF of X for Example 5.1.

Table 2: Statistical characteristics of the estimator of the probability of Example 5.1 (Case 1).

	relative bias(%)	coefficient of variation	average computational effort
SuS	-97.8	3.747	7,222
aE-SuS	3.5	0.376	5,970
MCS	0	4.093	5,970

Table 3: Statistical characteristics of the estimator of the probability of Example 5.1 (Case 2).

	relative bias(%)	coefficient of variation	average computational effort
SuS	/	/	/
aE-SuS	2.4	0.242	44,737
MCS	0	1.495	44,737

433 5.2. Multidimensional flow-based problem

434 In this example, the failure event is defined as

$$\sum_{i=1}^n X_i(1 - Y_i) \geq t \quad (11)$$

435 where X_i are independent and identically distributed (iid) according to the
 436 normal distribution $\mathcal{N}(\cdot; \mu, \sigma^2)$ and Y_i are also iid and follow the Bernoulli
 437 distribution $\text{Ber}(1 - p_{fc})$ with outcomes $\{0, 1\}$. Each X_i can be regarded as
 438 a loss variable associated to a failure event with probability p_{fc} . The failure
 439 event is further defined as the total loss exceeding the predefined threshold
 440 t . Let $\tilde{X}_i = -X_i \sim \mathcal{N}(\cdot; -\mu, \sigma^2)$, $\tilde{t} = -t$, and $\tilde{Y}_i = 1 - Y_i \sim \text{Ber}(p_{fc})$. The
 441 failure probability then becomes

$$\begin{aligned} p_f &= \mathbb{P} \left(\sum_{i=1}^n -X_i(1 - Y_i) \leq -t \right) = \mathbb{P} \left(\sum_{i=1}^n \tilde{X}_i \tilde{Y}_i \leq \tilde{t} \right) \\ &= \sum_{i=0}^n \mathbb{P} \left(\sum_{j=1}^n \tilde{Y}_j = i \right) \mathbb{P} \left(\sum_{k=1}^n \tilde{X}_k \tilde{Y}_k \leq \tilde{t} \mid \sum_{j=1}^n \tilde{Y}_j = i \right) \\ &= \sum_{i=1}^n \binom{n}{i} p_{fc}^i (1 - p_{fc})^{n-i} \Phi \left(\frac{\tilde{t} - (-\mu i)}{\sqrt{i \cdot \sigma^2}} \right) + (1 - p_{fc})^n \mathbb{I}(\tilde{t} \geq 0) \end{aligned} \quad (12)$$

442 Eq.(12) shows that the failure probability p_f is a function of n and \tilde{t} when
 443 fixing μ, σ and p_{fc} . For different n , we choose \tilde{t} such that the failure proba-
 444 bility equals to p_f^* . In this way, we define a series of failure events of different
 445 dimension but with the same failure probability, p_f^* . Note that there is a
 446 'jump' of value $(1 - p_{fc})^n$ at the origin coordinate; this value decreases as the
 447 dimension increases. Fig. 5 shows the failure probability p_f as a function of
 448 \tilde{t} for the case $n = 1$ (the dimension is 2) and $n = 50$ (the dimension is 100).
 449 The failure probability can also be regarded as the CDF of $\sum_{i=1}^n \tilde{X}_i \tilde{Y}_i$.

450 Next, MCS, standard SuS and aE-SuS are carried out to obtain the failure
 451 probabilities. SuS and aE-SuS are performed in standard normal space with
 452 aCS as the MCMC algorithm. Here, we set $p_{fc} = p_f^* = 10^{-3}$, $\mu = -10$, $\sigma = 1$
 453 and vary n from 1 to 50. tol , N_0 and p_0 for aE-SuS are set to be 0.5, 1,000, 0.1,
 454 respectively. As shown in Fig. 6, the computational cost of aE-SuS, which
 455 is measured by the total number of LSF evaluations, decreases rapidly with
 456 increasing dimension and reaches around 4,000 calls of the LSF for higher

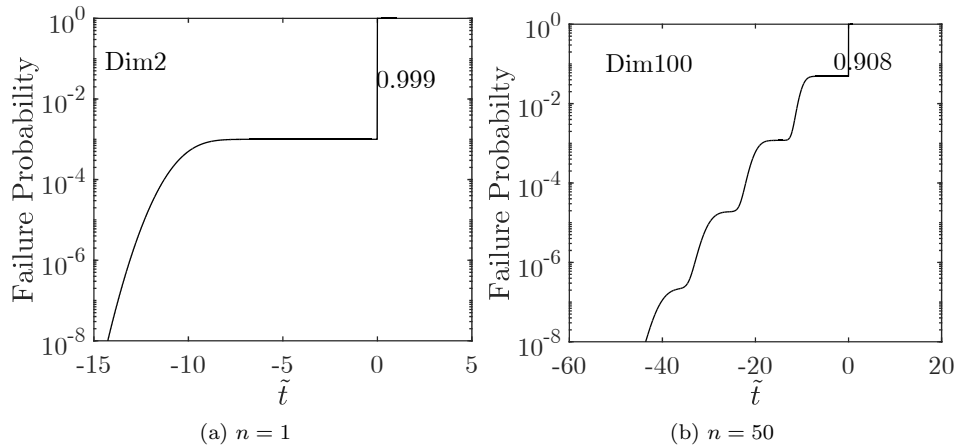


Figure 5: Failure probability p_f vs. \tilde{t} for the flow problem of Example 5.2.

457 dimensions. In order to obtain the statistical characteristics of the aE-SuS
 458 estimator and to compare them with MCS and standard SuS, 500 independ-
 459 ent trials of aE-SuS and SuS are carried out. The results of MCS are
 460 calculated theoretically with the same computational cost (total number of
 461 samples N_{tot}) as aE-SuS. The MCS estimator is unbiased and the coefficient
 462 of variation is $\frac{1-p_f}{\sqrt{N_{tot} \cdot p_f}}$. Fig. 7 and Fig. 8 illustrate the relative bias and the
 463 coefficient of variation of both aE-SuS and MCS. We see that the behavior
 464 of aE-SuS is similar to that of MCS in low dimensions where the jump at the
 465 origin is large, while in high dimensions where the jump of the CDF becomes
 466 smaller, aE-SuS is more efficient. We note that the influence of the number
 467 of random variables on the performance of the MCMC algorithm used in
 468 aE-SuS is insignificant. This is due to the fact that the aCS is especially
 469 designed for high dimensional problems.

470 Fig. 9 compares the square root of MSE (RMSE, calculated through esti-
 471 mates of the two terms of Eq.(4)) of aE-SuS with different settings of standard
 472 SuS. It can be seen that even with well-tuned parameters ($p_0 = 1/40$), stan-
 473 dard SuS can lead to significant errors in low to moderate dimensions where
 474 the jump in the CDF of the LSF is large.

475 As the 'jump' vanishes for large n , the results of aE-SuS become similar
 476 to that of standard SuS. In low dimensions, the aE-SuS algorithm behaves
 477 similar to crude MCS.

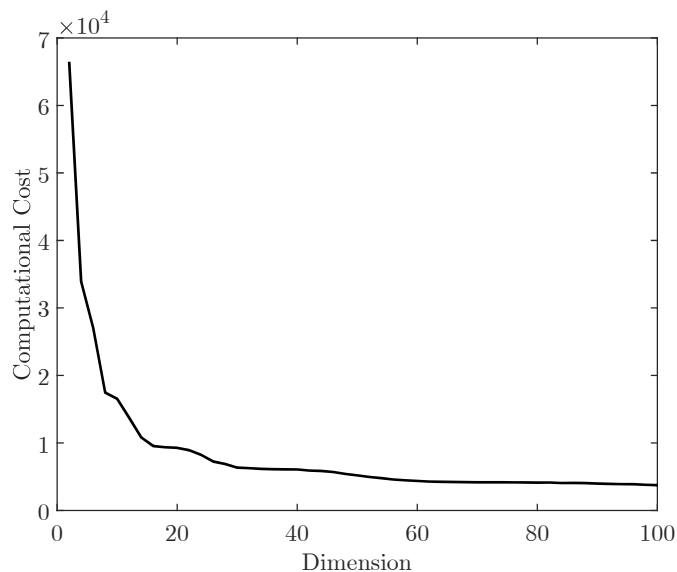


Figure 6: Computational cost of the aE-SuS for Example 5.2.

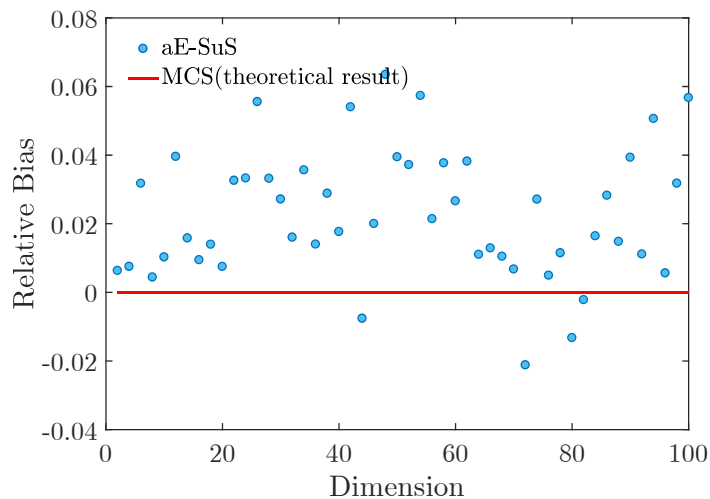


Figure 7: Relative bias (aE-SuS vs. MCS) for Example 5.2.

478 *5.3. Binomial experiment*

This example studies the behavior of the independent M-H algorithm proposed in Section 3.2. Consider a binomial experiment with n trials. Each trial is an independent event that has two outcomes: 0 and 1. The probability that a trial is successful (takes outcome 1) is equal to p and we evaluate the

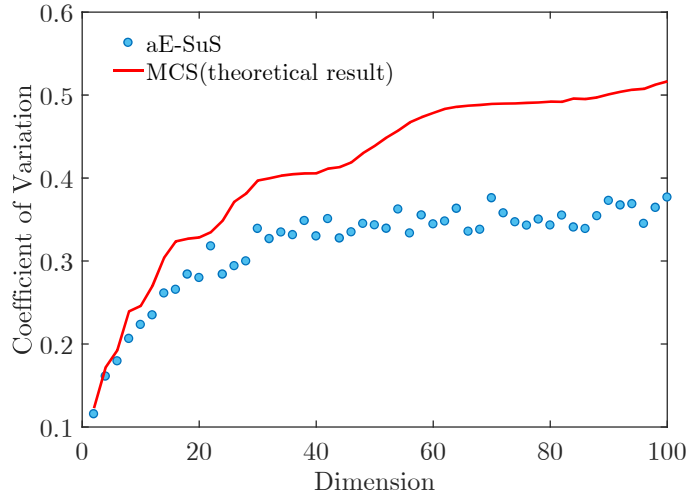


Figure 8: Coefficient of variation (aE-SuS vs. MCS) for Example 5.2.

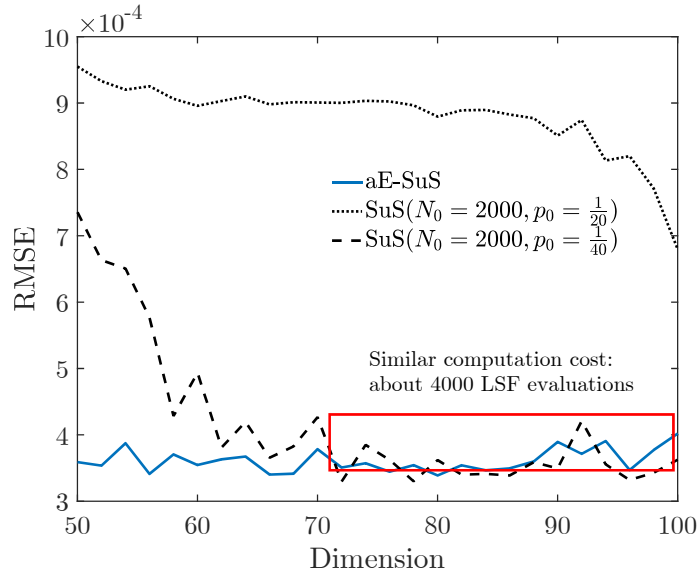


Figure 9: RMSE (aE-SuS vs. SuS) for Example 5.2.

probability that at least t trials are successful. The LSF is then defined as:

$$g(\mathbf{X}) = t - \sum_{i=1}^n X_i$$

479 where X_i represents the outcome of the i -th trial. The exact failure proba-
 480 bility can be expressed as $1 - F_B(t - 1; n, p_{fc})$ where $F_B(\cdot; n, p)$ is the CDF
 481 of the binomial distribution with parameters n and p .

482 In order to study the performance of the independent M-H algorithm in dif-
 483 ferent dimensions, we fix p at 10^{-3} and vary n . For each n , aE-SuS with the
 484 independent M-H algorithm is run 200 times with parameters $tol = 0.8, p_0 =$
 485 $0.1, N_0 = 2,000$.

486 For different dimensions and conditional levels of aE-SuS, the mean accep-
 487 tance rate of the independent M-H algorithm, $\mathbb{E}(\alpha)$, is calculated through
 488 Eq.(10) and is summarized in Table 4. Note that $\mathbb{P}(\mathbf{X} \in F_l)$ and $\mathbb{P}(\mathbf{X} \notin$
 489 $\cup_{i=0, \dots, l-1} \mathcal{X}_i)$ in Eq.(10) are abbreviated as $\mathbb{P}(F_l)$ and $\mathbb{P}(\overline{\cup \mathcal{X}_i})$, respectively.
 490 One can see that both $\mathbb{P}(F_l)$ and $\mathbb{P}(\overline{\cup \mathcal{X}_i})$ decrease as conditional level l in-
 491 creases. However, $\mathbb{P}(\overline{\cup \mathcal{X}_i})$ drops much slower than $\mathbb{P}(F_l)$ at high levels, which
 492 results in small $\mathbb{E}(\alpha)$. This is because, to form a good proposal in the inde-
 493 pendent M-H algorithm, the states that need to be excluded from the input
 494 distribution grow exponentially with l . This effect is more pronounced in
 495 high dimensions, leading to a faster decrease of $\mathbb{E}(\alpha)$. At the fourth level,
 496 the mean acceptance rate for $n = 100$ is only 0.2% of the rate for $n = 25$ in
 497 this example.

498 Nevertheless, if the mean acceptance rate is not too small, the independent
 499 M-H algorithm performs well. For instance, if we fix the threshold t at 4, the
 500 results of 200 independent runs of aE-SuS are summarized in Table 5. For
 501 all 4 cases, aE-SuS is slightly biased with less computational cost than crude
 502 MCS for achieving the same coefficient of variation. Note that the average
 503 computational cost for $n = 25$ is much higher than the other three cases,
 504 which is due to the larger 'jumps' in the CDF of the LSF.

505

506 5.4. Power network system

507 In this example, we consider the IEEE39 bus benchmark system, which
 508 consists of 39 nodes and 46 weighted edges. The topology of the network is il-
 509 lustrated in Fig. 10 where orange circles represent the source nodes and grey
 510 circles represent the terminal nodes. Edges are weighted by their reactance
 511 values shown on the right-hand side of Fig. 10 and by their capacities shown
 512 on the left-hand side. The line capacity is modeled here as being proportional
 513 to the number of most efficient paths between any source and terminal node
 514 pair passing through that line. This example was previously investigated by
 515 Scherb et al. [40] to quantify the network reliability considering cascading

Table 4: Mean acceptance rate of the independent M-H algorithm for Example 5.3.

		$n = 25$	$n = 50$	$n = 75$	$n = 100$
$l = 1$ $(g(\mathbf{X}) < t)$	$\mathbb{P}(F_l)$	0.025	0.049	0.072	0.095
	$\mathbb{P}(\cup \mathcal{X}_i)$	0.025	0.049	0.072	0.095
	$\mathbb{E}(\alpha)$	1	1	1	1
$l = 2$ $(g(\mathbf{X}) < t - 1)$	$\mathbb{P}(F_l)$	$2.95 \cdot 10^{-4}$	0.0012	0.0026	0.0046
	$\mathbb{P}(\cup \mathcal{X}_i)$	$2.95 \cdot 10^{-4}$	0.0012	0.0026	0.0046
	$\mathbb{E}(\alpha)$	1	1	1	1
$l = 3$ $(g(\mathbf{X}) < t - 2)$	$\mathbb{P}(F_l)$	$2.26 \cdot 10^{-6}$	$1.89 \cdot 10^{-5}$	$6.40 \cdot 10^{-5}$	$1.50 \cdot 10^{-4}$
	$\mathbb{P}(\cup \mathcal{X}_i)$	$2.26 \cdot 10^{-6}$	$1.89 \cdot 10^{-5}$	$1.87 \cdot 10^{-4}$	0.0017
	$\mathbb{E}(\alpha)$	1	1	0.34	0.087
$l = 4$ $(g(\mathbf{X}) < t - 3)$	$\mathbb{P}(F_l)$	$1.24 \cdot 10^{-8}$	$2.22 \cdot 10^{-7}$	$1.15 \cdot 10^{-6}$	$3.63 \cdot 10^{-6}$
	$\mathbb{P}(\cup \mathcal{X}_i)$	$1.24 \cdot 10^{-8}$	$9.70 \cdot 10^{-6}$	$1.84 \cdot 10^{-4}$	0.0017
	$\mathbb{E}(\alpha)$	1	0.023	0.0063	0.0021

Table 5: Statistics of the aE-SuS estimator for Example 5.3.

	$n = 25$	$n = 50$	$n = 75$	$n = 100$
p_f	$1.24 \cdot 10^{-8}$	$2.22 \cdot 10^{-7}$	$1.15 \cdot 10^{-6}$	$3.63 \cdot 10^{-6}$
relative bias(%)	2	3	5	2
coefficient of variation	0.15	0.14	0.20	0.34
average cost	$8.23 \cdot 10^4$	$3.77 \cdot 10^4$	$2.68 \cdot 10^4$	$2.09 \cdot 10^4$
MCS cost	$3.58 \cdot 10^9$	$2.30 \cdot 10^8$	$2.17 \cdot 10^7$	$2.38 \cdot 10^6$

516 effects and spatially distributed hazards, and by ro-Velasquez and Straub
 517 [41] to select representative failure scenarios.

The state of each node is considered as an independent Bernoulli random

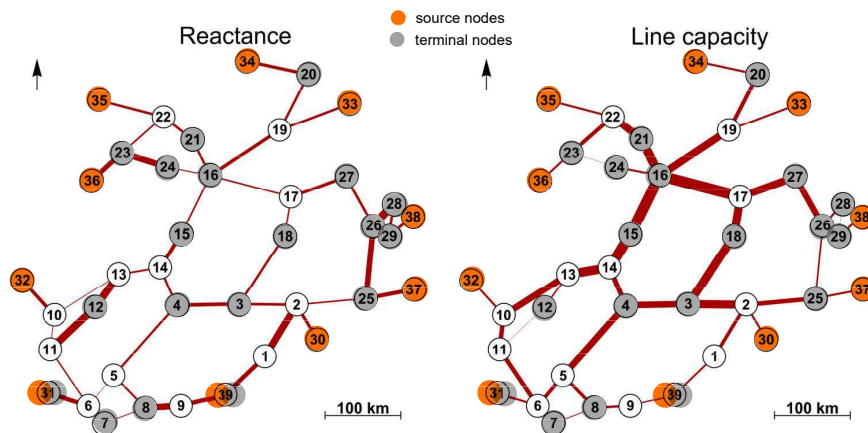


Figure 10: IEEE39 bus system, with edge thicknesses proportional to their estimated capacities (left) and reactances (right)[40].

518 variable, with component failure probability randomly chosen from the uni-
 519 form distribution $U[0, 10^{-2}]$. The LSF is then defined as a function of the
 520 system state \mathbf{x} , which is a binary vector, as follows:
 521

$$g(\mathbf{x}) = \frac{E(\mathbf{x})}{E(\mathbf{1})} - \text{threshold} \quad (13)$$

522

$$E(\mathbf{x}) = \frac{1}{|SN||TN|} \sum_{s \in SN, t \in TN, t \neq s} \text{eff}_{st}(\mathbf{x}) \quad (14)$$

523 eff_{st} is the efficiency of the most efficient path from source node s to terminal
 524 node t , which is evaluated as the inverse of the sum of the reactance values
 525 along that path. $E(\mathbf{x})$ is the efficiency of the whole system associated to the
 526 system state \mathbf{x} (The vector $\mathbf{1}$ is the intact system state). It is equal to the
 527 mean value of all the eff_{st} from each source node in set SN to each terminal
 528 nodes in set TN .

529 In order to model cascading effects, Eq.(13) is modified to

$$g(\mathbf{x}) = \frac{E(C(\mathbf{x}))}{E(\mathbf{1})} - \text{threshold} \quad (15)$$

530 where $\mathcal{C}(\mathbf{x})$ is the final system state after cascading effects due to overloading
531 of system components. These are triggered by overloading in individual lines
532 following initial failures, and are modeled following [40] and [42].

533 The threshold is fixed to 0.3, which means the system is considered as failed
534 when its efficiency is less than 30% of that of the intact system. We ap-
535 ply the aE-SuS algorithm in original Bernoulli space and set the parameters
536 $N = 2,000, p_0 = 0.1, tol = 0.8$. The MCMC algorithm is the independent
537 M-H algorithm. Fig. 11 shows the empirical CDF of $g(\mathbf{X})$ obtained by
538 MCS and the aE-SuS algorithm respectively. The aE-SuS algorithm is run
539 200 times to obtain the mean value, 10 percentile and 90 percentile of the
540 empirical CDF, while a single MCS run with 10^6 samples is carried out for
541 validation.

542 The average computational cost of aE-SuS is 9,507 calculations of the LSF
543 $g(\cdot)$ and the relative bias of the failure probability is 0.9%, while the coef-
544 ficient of variation is 0.338. To achieve the same coefficient of variation as
545 aE-SuS, crude MCS needs $1.74 \cdot 10^5$ calculations of the LSF in theory, which
546 is significantly larger than that of aE-SuS. The average CPU time over 200
547 repetitions of aE-SuS is reported as 682 seconds on a 3.50GHz Intel Xeon
548 E3-1270v3 computer. As a comparison, the CPU time for crude MCS with
549 $1.74 \cdot 10^5$ samples on the same machine is $9.83 \cdot 10^3$ seconds, which is about
550 14 times larger than the CPU time of aE-SuS.

551 The standard SuS algorithm is not applicable for this example due to the
552 large jump in the CDF of the LSF.

553 6. Conclusions

554 We introduce adaptive effort subset simulation, which enables solving
555 reliability problems with performance functions that follow a discontinuous
556 distribution. Such problems often occur in network reliability assessment be-
557 cause of discrete random variables appearing in the input random vector or
558 due to discontinuities in the function that defines the system performance.
559 The proposed method modifies the adaptive selection of the intermediate
560 domains of the standard SuS and adapts the number of samples and the
561 respective conditional probability throughout the simulation to ensure that
562 there is an adequate number of seeds at each level.

563 Any MCMC algorithm that enables efficient conditional sampling can be
564 combined with the proposed algorithm. We implement the aCS algorithm
565 in an underlying standard normal space. If the input random variables are

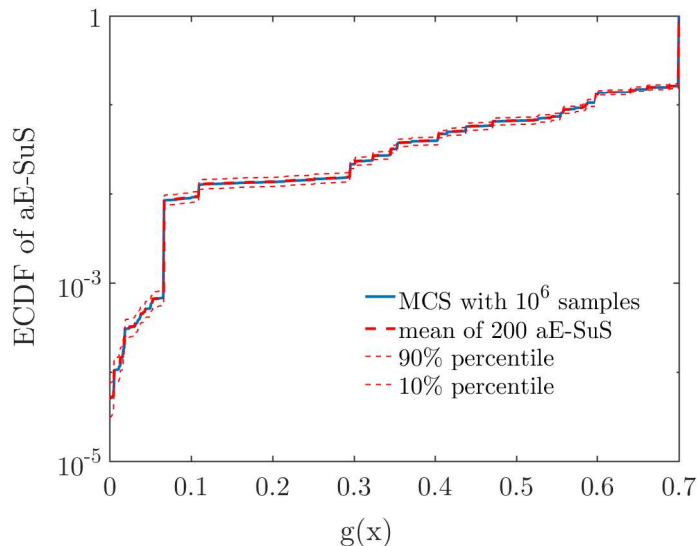


Figure 11: Results obtained by aE-SuS and MCS for IEEE39 network of Example 5.4.

566 all discrete, we propose a more efficient yet less general independent M-H
 567 algorithm, which operates in the original space. The mean acceptance rate
 568 of the independent M-H algorithm tends to decrease with increase of the in-
 569 termediate simulation level with decreasing rate depending on the dimension
 570 of the input space. Hence, the algorithm becomes inefficient in estimating
 571 small probabilities of high dimensional systems. The acceptance rate of the
 572 aCS algorithm is independent of the input dimension, however aCS performs
 573 worse than the independent M-H algorithm in moderate dimensional discrete
 574 input spaces.

575 Numerical results demonstrate that the aE-SuS estimator is only slightly
 576 biased and has substantially higher efficiency than crude Monte Carlo in
 577 problems where standard SuS fails to converge. The computational cost of
 578 the aE-SuS algorithm depends highly on the magnitude of the jumps in the
 579 distribution of the LSF.

580 7. Acknowledgment

581 The first author gratefully acknowledges the financial support of the
 582 China Scholarship Council.

583 **Appendix A. Adaptive conditional sampling algorithm**

584 The aCS algorithm presented herein differs from the one of [28], which
 585 assumes that $N = \frac{1-p_0}{p_0} N_{seed}$. N is the number of new generated samples
 586 and N_{seed} represents the number of seeds. The implementation of the aCS
 587 is summarized in Algorithm 4. In the algorithm, l is the intermediate level, and
 588 n is the dimension. F_l is the intermediate event. \mathcal{S}_l represents the seeds, and
 589 λ_{l-1} is the updated scaling parameter at the $l - 1$ -th level. It is suggested
 590 in [28] to choose λ_0 as 0.6. a^* , N_a , $\{\sigma_{0,d}\}_{d=1}^n$ are respectively the optimal
 591 acceptance rate, number of chains to consider for adaption, and the starting
 592 values for standard deviation. The suggested values can also be found in [28].

593 **Appendix B. Bound based sampling algorithm**

594 The original bound-based sampling algorithm [12, 8] is proposed for con-
 595 nectivity based problems in multivariate Bernoulli spaces. However, it can be
 596 modified to sample from the proposal distribution at level l of the indepen-
 597 dent M-H algorithm of Section 3.2, $Q_p^{(l)}(\mathbf{x}) \propto Q(\mathbf{x}|F_0)\mathbb{I}\{\mathbf{x} \notin \cup_{j=0,\dots,l-1}\mathcal{X}_j\}$,
 598 if the input random variables follow the multivariate categorical distribution.
 599 That is

$$Q(\mathbf{x}|F_0) = \prod_{d=1}^n \sum_{i=1}^{n_d} \mathbb{I}\{x_d = i\} \theta_{d,i} \quad (\text{B.1})$$

600 where $\theta_{d,i}$ represents the probability that the d -th component x_d equals value
 601 i given all preceding components x_1, \dots, x_{d-1} . n and n_d represent the number
 602 of components and the number of the states of x_d , respectively. For each
 603 component d , it holds that $\sum_{i=1}^{n_d} \theta_{d,i} = 1$.

604 The bound-based sampling algorithm proceeds in a component-wise scheme
 605 and is shown in Algorithm 5. Following this algorithm, one generates samples
 606 in the space $\{\mathbf{x} : \mathbf{x} \notin \cup_{j=0,\dots,l-1}\mathcal{X}_j\}$ with probability proportional to the input
 607 distribution $Q(\mathbf{x}|F_0)$. A detailed proof can be found in [8].

608

609 **References**

- 610 [1] K. M. Zuev, S. Wu, and J. L. Beck, “General network reliability problem
 611 and its efficient solution by subset simulation,” *Probabilistic Engineering*
 612 *Mechanics*, vol. 40, pp. 25–35, 2015.

Algorithm 4: Adaptive conditional sampling algorithm

Input: $N, F_l, \mathcal{S}^{(l)}, \lambda_{l-1}$
 1 $N_s \leftarrow |\mathcal{S}^{(l)}|, \lambda \leftarrow \lambda_{l-1}$
 2 Define $a^*, N_a, \{\sigma_{0,d}\}_{d=1}^n$ according to [28]
 3 Randomly sort the seeds $\mathcal{S}^{(l)}$
 4 Randomly choose $\text{mod}(N, N_s)$ elements from the set $\{1, 2, \dots, N_s\}$,
 say χ
 5 $\mathcal{P}^{(l)} \leftarrow \emptyset, c_1 \leftarrow 0, c_2 \leftarrow 0$
 6 **for** $i = 1, \dots, N_s$ **do**
 7 $\sigma_d \leftarrow \min(1, \lambda \sigma_{0,d}), \rho_d \leftarrow \sqrt{1 - \sigma_d^2}; \quad d = 1, \dots, n$
 8 **if** $i \in \chi$ **then**
 9 $j \leftarrow \lfloor \frac{N}{N_s} \rfloor + 1$
 10 **else**
 11 $j \leftarrow \lfloor \frac{N}{N_s} \rfloor$
 12 $\mathbf{u}_0 \leftarrow$ the i -th seed
 13 **for** $k = 1, \dots, j$ **do**
 14 **for** $d = 1, \dots, n$ **do**
 15 %% sample the d -th component of candidate \mathbf{v}
 16 $v_d \leftarrow \mathcal{N}(\cdot; \rho_d \mathbf{u}_{k-1,d}, \sigma_d^2)$
 17 **if** $\mathbf{v} \in F_l$ **then**
 18 $\mathbf{u}_k \leftarrow \mathbf{v}$
 19 $c_1 \leftarrow c_1 + 1, c_2 \leftarrow c_2 + 1$
 20 **else**
 21 $\mathbf{u}_k \leftarrow \mathbf{u}_{k-1}$
 22 $c_1 \leftarrow c_1 + 1$
 23 Add \mathbf{u}_k to $\mathcal{P}^{(l)}$
 24 **if** i is a multiple of N_a **then**
 25 $\lambda \leftarrow \lambda \exp((\frac{i}{N_a})^{-1/2} [\frac{c_2}{c_1} - a^*])$
 26 $c_1 \leftarrow 0, c_2 \leftarrow 0$
 27 $\lambda_l \leftarrow \lambda$
Output: $\mathcal{P}^{(l)}, \lambda_l$

Algorithm 5: Bound based sampling algorithm

Input: $Q(\mathbf{x}|F_0)$

```
1 for  $d = 1, \dots, n$  do
2   Calculate  $\Pr(\mathbf{x} \notin \cup_{j=0, \dots, l-1} \mathcal{X}_j | x_1, \dots, x_{d-1})$ 
3   for  $i = 1, \dots, n_d$  do
4     Calculate  $\Pr(\mathbf{x} \notin \cup_{j=0, \dots, l-1} \mathcal{X}_j | x_1, \dots, x_{d-1}, x_d = i)$ 
5      $\theta_{d,i}^* \leftarrow \theta_{d,i} \frac{\Pr(\mathbf{x} \notin \cup_{j=0, \dots, l-1} \mathcal{X}_j | x_1, \dots, x_{d-1}, x_d = i)}{\Pr(\mathbf{x} \notin \cup_{j=0, \dots, l-1} \mathcal{X}_j | x_1, \dots, x_{d-1})}$ 
6   Sample  $x_d$  from the categorical distribution  $\text{Cat}(x; \boldsymbol{\theta}_d^*)$ 
```

Output: candidate \mathbf{x}

- 613 [2] J. Ching and W.-C. Hsu, “An efficient method for evaluating origin-
614 destination connectivity reliability of real-world lifeline networks,”
615 *Computer-Aided Civil and Infrastructure Engineering*, vol. 22, no. 8,
616 pp. 584–596, 2007.
- 617 [3] M. Rausand and A. Hoyland, *System reliability theory: models, statisti-
618 cal methods, and applications*. John Wiley & Sons, 2003, vol. 396.
- 619 [4] G. S. Fishman, “A Monte Carlo sampling plan for estimating network
620 reliability,” *Operations Research*, vol. 34, no. 4, pp. 581–594, 1986.
- 621 [5] T. Elperin, I. Gertsbakh, and M. Lomonosov, “Estimation of network
622 reliability using graph evolution models,” *IEEE Transactions on Relia-
623 bility*, vol. 40, no. 5, pp. 572–581, 1991.
- 624 [6] H. Cancela and M. El Khadiri, “A recursive variance-reduction algo-
625 rithm for estimating communication-network reliability,” *IEEE Trans-
626 actions on Reliability*, vol. 44, no. 4, pp. 595–602, 1995.
- 627 [7] K.-P. Hui, N. Bean, M. Kraetzl, and D. P. Kroese, “The cross-entropy
628 method for network reliability estimation,” *Annals of Operations Re-
629 search*, vol. 134, no. 1, p. 101, 2005.
- 630 [8] P. L’Ecuyer, G. Rubino, S. Saggadi, and B. Tuffin, “Approximate zero-
631 variance importance sampling for static network reliability estimation,”
632 *IEEE Transactions on Reliability*, vol. 60, no. 3, pp. 590–604, 2011.

- 633 [9] L. Murray, H. Cancela, and G. Rubino, “A splitting algorithm for net-
634 work reliability estimation,” *IIE Transactions*, vol. 45, no. 2, pp. 177–
635 189, 2013.
- 636 [10] Z. I. Botev, P. L’Ecuyer, G. Rubino, R. Simard, and B. Tuffin, “Static
637 network reliability estimation via generalized splitting,” *INFORMS*
638 *Journal on Computing*, vol. 25, no. 1, pp. 56–71, 2013.
- 639 [11] R. Vaisman, D. P. Kroese, and I. B. Gertsbakh, “Splitting sequential
640 Monte Carlo for efficient unreliability estimation of highly reliable net-
641 works,” *Structural Safety*, vol. 63, pp. 1–10, 2016.
- 642 [12] G. Rubino and B. Tuffin, *Rare event simulation using Monte Carlo meth-*
643 *ods*. John Wiley & Sons, 2009.
- 644 [13] R. Paredes, L. Dueñas-Osorio, K. S. Meel, and M. Y. Vardi, “Princi-
645 pled network reliability approximation: A counting-based approach,”
646 *Reliability Engineering & System Safety*, vol. 191, p. 106472, 2019.
- 647 [14] G. S. Fishman, “The distribution of maximum flow with applications to
648 multistate reliability systems,” *Operations Research*, vol. 35, no. 4, pp.
649 607–618, 1986.
- 650 [15] —, “Monte Carlo estimation of the maximal flow distribution with
651 discrete stochastic arc capacity levels,” *Naval Research Logistics (NRL)*,
652 vol. 36, no. 6, pp. 829–849, 1989.
- 653 [16] G. S. Fishman and T.-Y. D. Shaw, “Evaluating reliability of stochastic
654 flow networks,” *Probability in the Engineering and Informational Sci-*
655 *ences*, vol. 3, no. 4, pp. 493–509, 1989.
- 656 [17] C. Alexopoulos and G. S. Fishman, “Characterizing stochastic flow net-
657 works using the Monte Carlo method,” *Networks*, vol. 21, no. 7, pp.
658 775–798, 1991.
- 659 [18] S. Bulteau and M. El Khadiri, “A new importance sampling Monte
660 Carlo method for a flow network reliability problem,” *Naval Research*
661 *Logistics (NRL)*, vol. 49, no. 2, pp. 204–228, 2002.
- 662 [19] J. E. Ramirez-Marquez and D. W. Coit, “A Monte-Carlo simulation
663 approach for approximating multi-state two-terminal reliability,” *Relia-*
664 *bility Engineering & System Safety*, vol. 87, no. 2, pp. 253–264, 2005.

- 665 [20] I. Gertsbakh, R. Rubinstein, Y. Shpungin, and R. Vaisman, “Permu-
666 tational methods for performance analysis of stochastic flow networks,”
667 *Probability in the Engineering and Informational Sciences*, vol. 28, no. 1,
668 p. 21, 2014.
- 669 [21] P.-C. Chang, “MC-based simulation approach for two-terminal multi-
670 state network reliability evaluation without knowing d-MCs,” *Reliability*
671 *Engineering & System Safety*, vol. 220, p. 108289, 2022.
- 672 [22] Y. Zhou, L. Liu, and H. Li, “Reliability estimation and optimisation
673 of multistate flow networks using a conditional Monte Carlo method,”
674 *Reliability Engineering & System Safety*, vol. 221, p. 108382, 2022.
- 675 [23] S.-K. Au and J. L. Beck, “Estimation of small failure probabilities in
676 high dimensions by subset simulation,” *Probabilistic engineering me-*
677 *chanics*, vol. 16, no. 4, pp. 263–277, 2001.
- 678 [24] W. Yu, W. Huang, K. Wen, J. Zhang, H. Liu, K. Wang, J. Gong, and
679 C. Qu, “Subset simulation-based reliability analysis of the corroding
680 natural gas pipeline,” *Reliability Engineering & System Safety*, vol. 213,
681 p. 107661, 2021.
- 682 [25] Z. I. Botev and D. P. Kroese, “Efficient Monte Carlo simulation via the
683 generalized splitting method,” *Statistics and Computing*, vol. 22, no. 1,
684 pp. 1–16, 2012.
- 685 [26] Z. I. Botev, P. l’Ecuyer, and B. Tuffin, “Reliability estimation for net-
686 works with minimal flow demand and random link capacities,” *arXiv*
687 *preprint arXiv:1805.03326*, 2018.
- 688 [27] Z. I. Botev and D. P. Kroese, “An efficient algorithm for rare-event prob-
689 ability estimation, combinatorial optimization, and counting,” *Method-*
690 *ology and Computing in Applied Probability*, vol. 10, no. 4, pp. 471–505,
691 2008.
- 692 [28] I. Papaioannou, W. Betz, K. Zwirgmaier, and D. Straub, “MCMC al-
693 gorithms for subset simulation,” *Probabilistic Engineering Mechanics*,
694 vol. 41, pp. 89–103, 2015.

- 695 [29] I. Papaioannou, S. Geyer, and D. Straub, “Improved cross entropy-based
696 importance sampling with a flexible mixture model,” *Reliability Engineering & System Safety*, vol. 191, p. 106564, 2019.
697
- 698 [30] R. Y. Rubinstein and D. P. Kroese, *Simulation and the Monte Carlo*
699 *method*. John Wiley & Sons, 2016, vol. 10.
- 700 [31] M. O. Ball, C. J. Colbourn, and J. S. Provan, “Network reliability,”
701 *Handbooks in operations research and management science*, vol. 7, pp.
702 673–762, 1995.
- 703 [32] J.-E. Byun and J. Song, “Generalized matrix-based Bayesian network
704 for multi-state systems,” *Reliability Engineering & System Safety*, vol.
705 211, p. 107468, 2021.
- 706 [33] J. He, “An extended recursive decomposition algorithm for dynamic seis-
707 mic reliability evaluation of lifeline networks with dependent component
708 failures,” *Reliability Engineering & System Safety*, vol. 215, p. 107929,
709 2021.
- 710 [34] W.-C. Yeh, “A quick bat for evaluating the reliability of binary-state
711 networks,” *Reliability Engineering & System Safety*, vol. 216, p. 107917,
712 2021.
- 713 [35] G. Hardy, C. Lucet, and N. Limnios, “K-terminal network reliability
714 measures with binary decision diagrams,” *IEEE Transactions on Relia-*
715 *bility*, vol. 56, no. 3, pp. 506–515, 2007.
- 716 [36] Z. Wang, M. Broccardo, and J. Song, “Hamiltonian Monte Carlo meth-
717 ods for subset simulation in reliability analysis,” *Structural Safety*,
718 vol. 76, pp. 51–67, 2019.
- 719 [37] S.-K. Au, “On MCMC algorithm for subset simulation,” *Probabilistic*
720 *Engineering Mechanics*, vol. 43, pp. 117–120, 2016.
- 721 [38] C. Andrieu and J. Thoms, “A tutorial on adaptive MCMC,” *Statistics*
722 *and Computing*, vol. 18, no. 4, pp. 343–373, 2008.
- 723 [39] W. R. Gilks and P. Wild, “Adaptive rejection sampling for gibbs sam-
724 pling,” *Journal of the Royal Statistical Society: Series C (Applied Statis-*
725 *tics)*, vol. 41, no. 2, pp. 337–348, 1992.

- 726 [40] A. Scherb, L. Garrè, and D. Straub, “Reliability and component im-
727 portance in networks subject to spatially distributed hazards followed
728 by cascading failures,” *ASCE-ASME Journal of Risk and Uncertainty*
729 *in Engineering Systems, Part B: Mechanical Engineering*, vol. 3, no. 2,
730 2017.
- 731 [41] H. Rosero-Velásquez and D. Straub, “Representative natural hazard sce-
732 narios for risk assessment of spatially distributed,” in *The 29th European*
733 *Safety and Reliability Conference*, 2019, pp. 1–7.
- 734 [42] P. Crucitti, V. Latora, and M. Marchiori, “Model for cascading failures
735 in complex networks,” *Physical Review E*, vol. 69, no. 4, p. 045104, 2004.